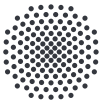

University of Stuttgart
Germany

Institute for Visualization and Interactive Systems
Universitätsstraße 38
70569 Stuttgart

Research Project-INFOTECH

An Adaptive Model of Gaze-based Selection

Jayakumar Ramasamy Sundararaj

Course of Study:	INFOTECH
Examiner:	Prof. Dr. Andreas Bulling
Supervisor:	Anna Penzkofer, M.Sc.
Commenced:	April 3, 2023
Completed:	August 31, 2023

Abstract

The emergence of gaze-based selection in the field of human-computer interaction has been a subject of considerable interest over time. Though notable progress has been made, there remains untapped potential for further advancements, particularly in deepening our understanding of the adaptive mechanisms governing eye movement and vision. This research is based on previous work , which introduces an innovative computational model aimed at explaining the details of gaze-based selection and the precise control of eye movements. The model we develop emulates the planning process involved in eye movements, enclosing critical aspects such as saccades, fixations, and the pivotal dwell phase leading to target selection. By formulating the model as an optimal sequential planning problem, we account for the constraints imposed by the human visual and motor systems. Using reinforcement learning techniques, the model approximates optimal solutions for the detailed sequence of eye movements that constructs gaze-based selections. Furthermore, this model successfully reproduces prior observations concerning the influence of target size and distance, effectively encapsulating a broad spectrum of performance aspects within gaze-based selection. A distinguished feature of our developed model is its unique capability to incorporate fixational eye movements (jitters), a facet unaddressed in previous work, thus enhancing the model's comprehensiveness. Through this model, we gain the capability to predict the number of fixations required and the duration for achieving successful gaze-based selections. In summary, our effort involves emulating the described baseline model, which aims to forecast the eye movement strategies essential for accomplishing gaze-based selections. In addition to this replication, we introduce a novel layer of jitter adaptiveness, enhancing the model's ability to effectively track the target's selection criterion.

Contents

List of Figures

1 Introduction

Human-computer interaction (HCI) has been rapidly evolving with advancements in technology. One such advancement is the development of Gaze-based interaction since the early 1990s. Gaze-based interaction allows users to interact with machines using eye movements. Gaze input is a feasible modality for hands-free interaction as it is fast and intuitive. It also provides more context-sensitive interaction than conventional methods, as our point of gaze often enacts the focus of visual attention [MB14]. This relation between the point of gaze and visual attention is crucial for comprehending how individuals process visual stimuli and interpret their environment. Over the years, advances in eye-tracking technology, especially in virtual and augmented reality (AR) systems, have renewed interest in this field [SMMZ19]. However, despite its promising prospects, comparing the performance of gaze input with traditional input methods like a mouse or touch input has led to conflicting results. Even though some studies suggested that gaze input was faster than head-pointing, others revealed that it was slower than the latter [HRMB18; QT17].

The apparent discrepancies arise due to the lack of a quantitative model developed specifically for gaze-based tasks. The lack of comprehensive models has made it difficult to draw firm conclusions from different experimental circumstances, where relatively minor factors of the design, such as viewing distance or tracking latency, can have a substantial impact on findings. In this setting, the development of comprehensive theories of gaze-based selection becomes critical to better understand the underlying causes of these variances [CAOH21]. Tatler et al. [TBC17] revealed that the robust theories about gaze-based tasks were centralised on temporal aspects rather than combining both the temporal and spatial aspects. In other words, existing modelling efforts have primarily centred on motor constraints, often neglecting the constraints stemming from the vision which is in accordance with Fitts' law. The study by Gori et al. [GRGB18] disclosed how experiments that use Fitts' law could lead to false conclusions.

To address these challenges and shed light on the adaptive mechanisms governing eye movement control during gaze-based selection, this research analyses and extends a novel adaptive model proposed by [CAOH21]. This computational model leverages a reinforcement learning algorithm to identify an optimal policy based on human-like bounds on motor movement and visual observations. The hypothesis is that eye movements are boundedly optimal, aiming to optimize utility functions while considering the properties of both the motor and visual system constraints [GHT15; HLV09; LHS14].

A distinctive aspect of our model lies in its adaptive eye movement strategies, which are shaped by a range of constraints, including target distance, target size, ocular-motor saccade noise, estimation noise in peripheral vision, and fixation jitter. These constraints give rise to a multi-step gaze-based selection process, which aligns with typical human behaviour. However, under certain circumstances, our model predicts one-step or even multi-step selections, offering insights into the variations of eye movement behaviour during selection. To evaluate the effectiveness of our model, we focus on replicating standard empirical findings relevant to enhancing gaze-based selection techniques

[SMMZ19]. Specifically, we aim to reproduce the effects of target size and distance and explore phenomena related to dwell-based selection [SMMZ19; ZRZ10]. Subsequently, we delve into the exploration of these developments through the framework of reinforcement learning. The learner tackles a Partially Observable Markov Decision Process (POMDP) with an observation function that adheres to the outlined constraints. By engaging in a trial-and-error process within a simulated environment, the model refines its understanding of the problem and the model becomes capable of predicting the target selection time and the average number of saccades made based on target size and eccentricity.

This research contributes to the advancement of gaze-based selection techniques and offers a deeper understanding of the underlying mechanisms governing eye movement control. By building on previous research in reinforcement learning and deep learning for modelling human-computer interaction, our model opens up new ways for exploring the adaptability and efficiency of gaze-based interactions in various HCI contexts. Through rigorous testing and validation against empirical data, our work aims to shed light on the adaptive nature of gaze-based selection and enhance the design and implementation of more sophisticated and user-friendly human-computer interfaces. By bridging the gap between theory and empirical findings, we seek to contribute to the ongoing progress in gaze-based interaction research and shape the future of HCI.

2 Related Work

Over the past few decades, gaze-based selection has become an increasingly popular technique for human-computer interaction. It enables users to interact with computers by directing their gaze at different elements on the screen. Studies are attempted to improve the efficiency of gaze-based selection methods. However, a better understanding of gaze-based selection techniques involves predicting the process that guides eye movement and vision. Regulation of eye movement mostly results in a sequence of saccades and fixation trailed by target selection using dwell time. In this literature review, we will identify key factors that influence gaze-based selection and shed light on existing research. By synthesizing the existing research on this topic, we hope to provide insights into how adaptive models of gaze-based selection can be modelled with human-like bounds on motor and visual systems.

2.1 Gaze-based Selection

Ware and Mikaelian [WM86] performed the first methodological analysis to report that eye gaze as an input modality is faster than other input types like mouse and touch input, especially when paired with a hardware button to confirm the selection. Since then, work in this field has focused on comparing gaze input to conventional input methods, yielding conflicting results [SMMZ19]. Hansen et al. [HRMB18] conducted an experiment to compare gaze and head-based pointing tasks to the mouse-pointing task. They reported that gaze and head-pointing inputs were equally fast but slower than mouse-pointing. The authors found that throughput for mouse input was the highest followed by head-pointing and gaze-pointing. The study from Zhang and Mackenzie also proved that the throughput for gaze-based selection was lower than the other selection methods [ZM07]. In the context of gaze-based selection, throughput refers to the rate at which a user can accurately and efficiently interact with a computer system using their gaze. It is a measure of the effectiveness and efficiency of the gaze-based interaction method. On the other hand, a study by Blattgerste et al. [BRP18] suggested that eye-gaze input for a larger field of view (FOV) is faster than head-based pointing inputs. Sibert and Jacob [SJ00] demonstrated that selecting a target with eye gaze was faster than with a mouse in terms of selection time.

Gaze-based selection depends not only on the time required to search for the target but also on the time to commit to the selection. These are termed Eye Movement Time (EMT) and dwell time respectively. Wu et al. [WKK10] suggested that the eye movement time depends on target size and target eccentricity. Saccadic eye movements play another important role in determining eye movement time. Saccades are typically small, ballistic movements that occur multiple times per second. They can be voluntarily or involuntarily initiated. In gaze-based selection tasks, voluntary saccade movements are mostly used to reach the target. The number of saccades required to reach a

target increases with a decrease in the target size and an increase in the target distance. This, in turn, increases the selection time because, for smaller and further targets, where a corrective saccade in addition to a primary saccade is required [SMMZ19; WKK10].

Apart from EMT, the performance of the gaze-based selection task depends heavily on the dwell time that is required to make the selection. Studies show that the dwell time must be at least as long as the dwell criterion to avoid the Midas touch problem: a problem that is defined by the selection of an entity other than our target while the gaze points to that entity for a short period of time [SMMZ19]. This is a generic problem because the eyes are perceptual organs and humans are not familiar with controlling them to provide inputs [MB14]. Gaze-based selections that require dwell time will allow users to point and select in the same way as using a mouse [FMK20]. The dwell criterion mentioned above refers to the amount of time that a user must fixate their gaze on a target in order for it to be selected. Consequently, a low dwell criterion leads to unintended selections and a high dwell criterion makes the selection of smaller targets impossible due to uncontrolled jitters in fixations. Studies reporting dwell times that are used in experiments include 50ms, 150ms, 200ms and up to 800ms [CAOH21]. There are works being attempted to reduce dwell time. One similar work from Isomoto et al. [IAST18] demonstrated the usage of Fitts' law to minimize dwell time. Their technique involved acquiring a target by comparing the difference between eye movement time estimated by Fitts' law and the actual measured eye movement time to a threshold value. The target is considered to be acquired if the calculated time is smaller than the threshold value. This reduced the average dwell time to 86.7ms with a 10.0% Midas touch rate.

2.2 Fitts' Law - An Incomplete Description of Gaze Interaction Dynamics

Researchers hypothesize that gaze-based selection tasks partially depend on Fitts' law [Fit54], where the time required to reach a target is dependent on the function of the ratio of target distance and target width. Fitts' law can be formulated as follows:

$$MT = a + b \log_2 \left(\frac{2D}{W} \right) \tag{2.1}$$

where,

- MT is the movement time or the time it takes to complete the selection.
- D is the distance between the starting point and the target location.
- W is the width of the target or the size of the object that the movement is aiming at.
- a and b are regression constants.

The logarithmic term in Fitts' law is commonly referred to as the Index of Difficulty (ID) [SMMZ19]. This is a measure of how difficult the task would be and is calculated as follows:

$$ID = \log_2 \left(\frac{2D}{W} \right) \tag{2.2}$$

This means that as the ID increases, MT also increases, indicating that the task takes longer and is more difficult to perform. The study by Crossman and Goodeveand validated that Fitts' law works well for target-directed movements under continuous motor control [CG83]. That, being said, saccadic eye movements are also target-directed and hence Fitts' law should be a gold standard in evaluating the gaze duration but studies are more divided on the applicability of Fitts' law to model gaze duration. While Miniotas et al. [Min00] reported a good fit of $r^2 = 0.98$, Zhai et al. [ZMI99] reported a lower fit of the order $r^2 = 0.72$. In addition, Sibert et al. [SJ00] showed that movement times were better predicted by just saccade amplitudes. One among many, a study by Schuetz et al. [SMMZ19] demonstrated the reason for this discrepancy in detail. A fundamental difference between saccadic eye movements and other pointing input methods is that eye movements cannot be reprogrammed based on new visual information. Without continuous feedback, the prediction of Fitts' law may not hold as accurately. Furthermore, the saccade duration or movement time is totally decided by the saccade amplitude independent of the target size. The saccade duration can be quantitatively calculated with the following equation [BSKH75]:

$$D = 37 + 2.7A \tag{2.3}$$

where D is the saccade duration and A is the amplitude of the saccade in terms of visual angle in degrees between two successive fixations.

On the other hand, the discrepancy in modelling gaze duration by just using saccade amplitudes could be resolved by considering target selection as a sequence of primary and secondary saccades. Humans frequently generate secondary ('corrective') saccades for smaller targets with high ID. Wu et al. [WKK10] demonstrated that movement times for a sequence of saccades followed Fitts' law. They revealed that the total movement time increased as the ID increased. This increase in time was linked to a greater occurrence of secondary saccades for smaller targets, while the main saccades were not affected in terms of their onset time and duration, and were primarily determined by the movement amplitude. This implies the likelihood of corrective saccades increases with the targets of higher ID. In order to model a gaze-based selection by Fitts' law, an occurrence of a primary and secondary or corrective saccade is required. Though the findings from [LD10; LT15] are not specifically related to studying gaze as a method of interaction, it aligns with the theories about pointing movements that are based on sub-movements and support the above statement.

2.3 POMDP Models of Gaze-based Selection

The number of saccades needed to complete a task is an emergent consequence of adaptation to the task environment and the limitations of human motor and visual systems. The constraints imposed by the human motor and visual system concern saccade and fixation latencies and also the decrease in visual sharpness with an increase in eccentricity from the centre of the visual field (fovea) towards the periphery [KH14]. Hence, the model developed should adapt to these constraints. Studies [BM08; CBB+15; CSBH17; HCAL18] suggest a way to model the gaze-based selection task as a sequential decision-making process and a Partially Observable Markov Decision Process (POMDP) is that type of decision-making framework that takes the uncertainty of an environment into account. However, modelling gaze-based selection as a POMDP is a relatively new approach that has gained increasing attention in recent years. POMDPs offer a systematic and logical way to analyze how an agent's actions and observations influence its understanding of the environment. Moreover,

a POMDP is a mathematical framework for modelling decision-making problems in which the agent's state is not directly observable and must be inferred from a sequence of noisy observations. POMDPs are preferred over Markov Decision Processes (MDP) because human visual search is inherently a partially observable task. When searching for a target object, humans often have incomplete information about the state of the environment, as they are only able to observe a limited portion of the scene at any given time. As a result, their perception of the environment is noisy and uncertain. Using an MDP to model human visual search would oversimplify the task, and the resulting model would not accurately reflect the challenges that humans face when searching for a target object in a visual environment. Earlier, Howes et al. [HCAL18] presented a POMDP model to help decision-making by employing eye movements to gather information from a data display. The model employed a sequence of incomplete observations gained through ocular fixations, progressively accumulating enough information from the visualization to make a conclusion.

POMDPs have been used in Cognitive Science to better understand human behaviour, such as in a study by Butko et al. [BM08] that looked at how individuals identify visual targets by shifting their eyes to obtain information. They framed this task as a POMDP and developed a model that learned a series of eye movements to maximize reward. Rao's model [Rao10] proved that the primate decision-making process could be described as a reward-maximizing solution to a POMDP, with the model determining the ideal threshold for transitioning from information gathering to decision-making.

2.4 Background - Reinforcement Learning

Reinforcement learning is a sort of machine learning in which an agent learns an optimal policy through experiences rather than examples, as in typical machine learning methods. The algorithms use rewards to select actions that maximize the reward over time. The agent in principle must interact with the real environment during training, however, this is not always a suitable approach, because in many scenarios making the agent learn from bad experiences might endanger the agent. This resulted in the agent being trained in a virtual environment before being tested in a real-world setting. During training, the agent interacts with the environment and selects an action depending on its present state; the agent learns the effectiveness of the action through the use of the reward function. The agent's goal is to learn a strategy that will instruct the agent on which action to take based on its current state. This strategy is called the policy and the agent attempts to learn a policy that will maximize the cumulative rewards at the end of each episode.

The solution to the POMDP problem is attained by learning an effective policy using the deep reinforcement learning method (Deep RL). Deep RL is a subset of reinforcement learning that employs deep neural networks to approximate the best action-value function or policy function. In other words, it is a hybrid of reinforcement learning and deep learning. Deep RL is commonly utilized in complicated situations with high-dimensional state and action spaces, where regular RL algorithms may fail to develop an effective policy. One such algorithm used here is the Proximal Policy Optimization algorithm (PPO). It uses a deep neural network to represent the policy or value function, and it optimizes the objective function using gradient descent. PPO is an evolution of prior policy optimization approaches such as TRPO (Trust Region Policy Optimization) [SLM+17], which also uses deep neural networks to represent the policy and/or value function. TRPO was data efficient and ensured to not have any policy degradation by optimizing the learning rate. However, it

added constraints to the objective function making it a quadratic optimization problem. PPO, on the other hand, adds significant adjustments to the objective function and the optimization algorithm that make it more sample-efficient and stable than earlier techniques. Equation 2.4 describes the objective function used in PPO [SWD+17].

$$L^{\text{CLIP}}(\theta) = \widehat{E_t}\left[\min\left(r_t(\theta)\widehat{A_t}, \text{clip}\left(r_t(\theta), 1-\varepsilon, 1+\varepsilon\right)\widehat{A_t}\right)\right] \tag{2.4}$$

The objective function of the Proximal Policy Optimization (PPO) algorithm combines two terms: the objective term from the Trust Region Policy Optimization (TRPO) algorithm and a clipped policy gradient term. The policy gradient term is clipped based on the advantage value, which represents the advantage of taking a particular action compared to others. PPO employs careful clipping to ensure that the policy update is conservative yet effective. When the advantage value is positive, the policy gradient term is clipped by $1 + \varepsilon$, and when it is negative, it is clipped by $1 - \varepsilon$. This means that updates to the policy for actions with positive advantages are limited to prevent large deviations, while actions with negative advantages have their updates restricted to avoid worsening the current policy. By adopting this approach, PPO guarantees that it takes small and safe steps towards identifying and reducing the impact of unfavourable actions while minimizing the influence of beneficial actions on the policy update. This cautious yet efficient updating strategy helps maintain the stability and performance of the learning process, ensuring that the algorithm avoids drastic changes that could harm the overall policy.

Once the model is developed considering the factors mentioned above, the behaviour of the model is compared with human data collected in factual studies published at CHI [SMMZ19]. The evaluation of the model is made by comparing various factors such as (1) the effect of target size on selection time (2) the effect of target size on the number of saccades (3) the effect of Index of Difficulty on the number of saccades, to the empirical findings made by Schuetz et al. [SMMZ19].

3 Methodology

This section aims to describe in detail the concept of problem formulation of gaze-based selection as POMDP and the RL approach adopted to solve the formulated problem. This methodology is based on the study by Chen et al. [CAOH21]. In addition to their efforts, we implemented a new feature known as jitter adaptiveness to the model. The subsections briefly describe the jitter feature as well as the assumptions made, the problem description and the implementation.

3.1 Gaze-based Selection Task

Chen et al. [CAOH21] showed that the strategies employed in gaze-based search and selection are a product of both environmental factors, such as target distance and width, and the limitations inherent in human visual-motor mechanisms. These constraints involve motor noise within the ocular motor system, spatial uncertainty in peripheral vision, the ballistic nature of eye saccades, and the irregularities introduced during fixation (jitters). To model the adaptation to these constraints, our approach treats gaze-based selection as a problem of sequential decision-making. We cast this problem as a POMDP and employ deep RL techniques to derive an optimal gaze search and selection strategy. This approach operates under the assumption that the decision of where to direct one's gaze is guided by the task's reward and cost structure. Thus, more effective gaze search patterns, aligning with desirable eye movement strategies, are reinforced through higher rewards.

3.1.1 Control in Gaze-based Selection

As shown in Figure 3.1, adapted from Chen et al. [CAOH21], the task entails a sequential interplay of eye movements, partial information gathering, and adjustments influenced by motor and visual system uncertainties, leading to the eventual accurate selection of the target. The user is required to shift their gaze towards a designated target, represented as a black circle, through a series of discrete saccade and fixation steps. In the provided illustration, the initial point of fixation is marked as location 1 (numbered in black). During this fixation, an observation is made using peripheral vision, characterized by lower visual acuity, resulting in a partially imprecise and noisy estimate, indicating that the target is situated at location 2. Subsequently, an eye movement is directed towards location 2, but due to inherent motor system noise, the eyes ultimately fixate on location 3. Now, with the fixation being closer to the target, a more precise estimate of the target's location (referred to as location 4) is generated. The eyes are aimed at location 4, but they ultimately end up fixated on location 5. After a brief dwell period, the final target selection takes place. In this case, the gaze-based selection is a two-step process (numbered in red colour).

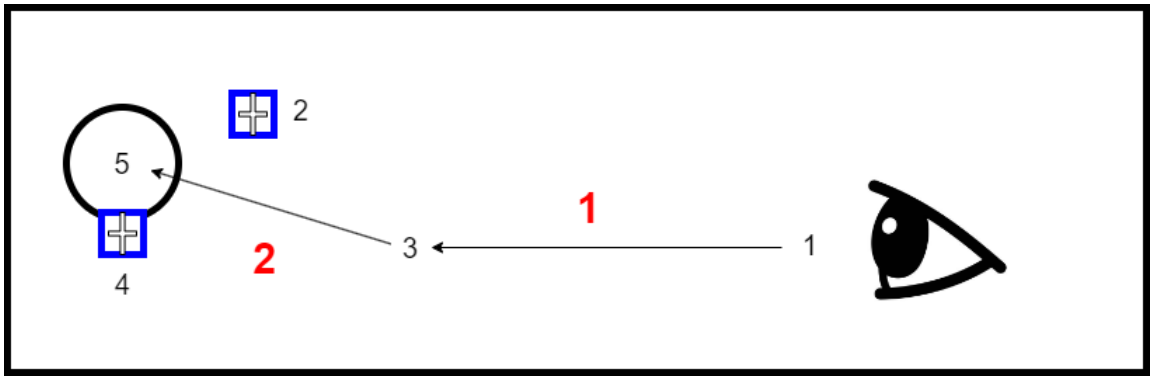

Figure 3.1: Control problem illustration in gaze-based selection. The user executes a sequence of two saccades (indicated by red numbers) to accurately reach the intended target at location 5. The blue crosses represent the user's perceived target positions – one after the initial fixation at 2, and the other after the first saccade at 4.

Gaze-based selection happens through a series of saccades and fixations. A saccade is a rapid movement that redirects the gaze from one point to another and during fixations, the eye positions are relatively stable. When the observer is instructed to search for and fixate on a target immediately upon its appearance, the onset latency represents the interval between the target's appearance and the initiation of the first saccade movement. Typically, the onset latency for the initial saccade is approximately 200 ms [FR84] and we made use of this in our model.

Fixational eye movements, often referred to as 'jitters', are small involuntary eye movements that occur even when we try to fixate on a stationary object. 'Microsaccades', 'Dwell drifts' and 'Tremors' are the three major types of fixational eye movements [Duc18]. Here, we focus on how dwell drifts affect the target selection time. For instance, during fixation on a small target region measuring 1.2° of visual angle, these jitters cause the gaze to intermittently exit and then re-enter the designated target area, leading to an effective duration of 1075 ms for a target that initially required a dwell of 800 ms [ZRZ10]. In our model, once the gaze fixates initially on the target, we introduced a simulated drift effect during the period of fixation. This drift (jitter) was created by generating location samples with some random noise, confined within an average jitter radius (denoted by AR) centred around the target's position [ZRZ10]. This assumption was grounded in the notion that participants in a real-world scenario tend to maintain their gaze close to the centre of the target, to reduce the time spent in fixation, thereby facilitating the activation of the selection process.

3.2 Model Implementation

As previously mentioned, we frame the gaze-based selection problem as a Partially Observable Markov Decision Process (POMDP)[CAOH21]. At every time step, the environment finds itself in one of several possible states. A state represents a possible target position. Initially, the agent lacks complete knowledge about the true state of the environment; it has access to only partial observations of it. Usually, the agent starts with a certain understanding of the situation and then takes an action that affects the environment's state. However, in our situation, the environment's

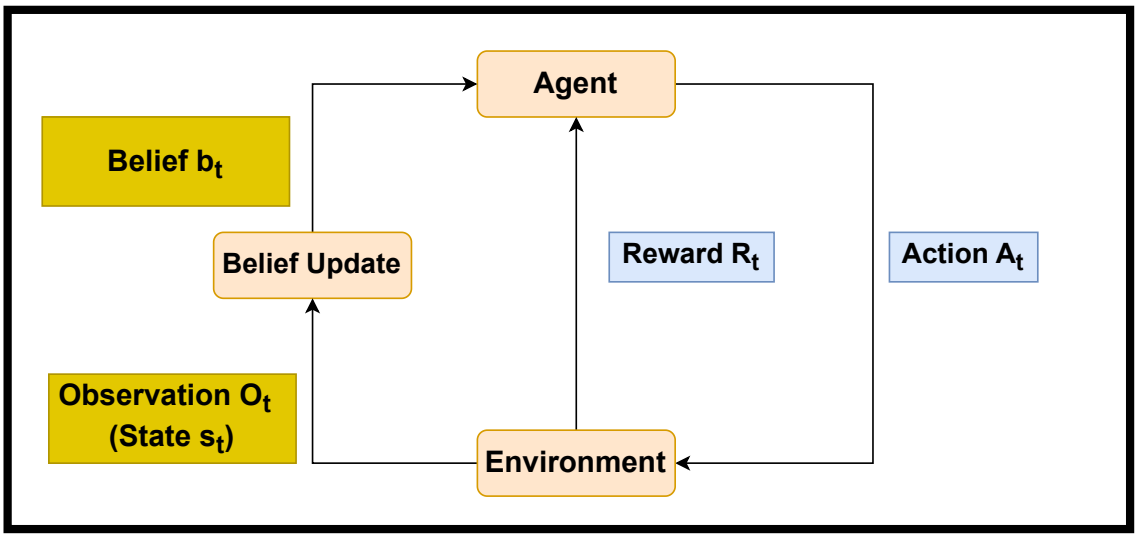

Figure 3.2: Structure of the model. The agent selects an action (saccade) based on its current target belief. The environment updates the state, providing a new fixation and partial observation to update the belief. Simultaneously, the reward function updates the agent's policy based on the action and new state.

state remains constant as the target position does not change in each episode, but our agent's belief of the state changes. The action's consequences are twofold. Firstly, the agent gains a new observation, which it employs to revise its current belief about the state, thus updating it to a fresh belief. Simultaneously, the agent receives a reward signal, the magnitude of which depends on both the environment's state and the specific action executed by the agent.

The reward function $r_t(s_t, a_t)$ generates rewards in response to the actions taken by the agent, based on the environment's current state s_t. If the agent successfully reaches the target region, the reward is 0. However, for each additional saccade made, a penalty of -1 is incurred. The primary goal is to maximize this reward system, encouraging the model to rapidly locate the target while adhering to the specified constraints.

Figure 3.2 depicts the overall RL process. The agent performs actions (saccades) based on its existing understanding of the target's location. The environment responds by updating the state, leading to a new fixation and providing a partial observation (O_t), which in turn allows the agent to revise its belief (b_t). Simultaneously, the reward function (R_t) modifies the agent's policy based on the action taken and the resulting new state. This cycle of action, observation, and reward continues iteratively until the selection process is completed, and the task is fulfilled. Essentially, the objective is to derive the optimal policy, a strategic set of actions that ensures the most appropriate outcome throughout the entire cycle, encompassing belief formation, action selection, and eventual task fulfilment. The definition of the POMDP in accordance with the structure of our model is discussed below.

In more detail, at each time step t, the environment occupies a specific state s_t where $s_t \epsilon S$, which represents a potential target position. This state is denoted as $s = [x, y]$, where both x and y values fall within the range of -1 to 1, effectively covering the display's edges. In each episode, the agent starts by fixating on the origin $[0, 0]$. A circular target with a diameter (W) is then introduced at a

distance (D) away from the starting point at a random angle (theta). Consequently, the state consists of a real-valued coordinate pair (x, y) that signifies the target's position, where $x = D \times cos(theta)$ and $y = D \times sin(theta)$. The state remains the same within each episode and is chosen randomly with a random angle θ across episodes.

In every episode, the agent needs to reach the randomly selected target by performing an action (saccade) at each time step. An action is represented as $a_t = [x, y]$, where both x and y values are within the range of -1 to 1. However, it's important to note that the accuracy of the aim saccade is impacted by *ocular motor noise*. Ocular motor constraints encompass the inherent limitations placed upon eye movement and gaze patterns due to physiological factors. These constraints play a crucial role in determining the trajectory of eye movements and the focal point of gaze during various tasks and activities. An essential constraint arises from the anatomical characteristics and physiological functioning of the eye itself. In the effort to model ocular motor noise, Chen et al. [CAOH21] adopted a widely accepted physiological assumption, known as signal-dependent noise (SDN). SDN constitutes zero-mean, white Gaussian noise that varies based on the magnitude of the signal. Therefore, the gaze position after a saccade is sampled from $\hat{a}_t \sim N(a, \sigma_{\text{ocular}}(t))$, where ocular motor noise exhibits a linear dependence on the saccadic amplitude [CAOH21]: $\sigma_{\text{ocular}}(t) = \rho_{\text{ocular}} \times \text{Amplitude}(t)$. Here, $\rho_{\text{ocular}} = 0.07$, is a hyper-parameter of the model taken from the experiments by Chen et al [CAOH21].

An observation o_t is received after the agent executes an action, and the observation of the target position is influenced by the true target location s_t, as well as the current fixation location a_t. However, human vision has the highest clarity in the fovea, which only covers around 1° - 2° of visual angle [Duc18]. Beyond this central area, acuity decreases significantly as eccentricity increases. Therefore, the observation o_t is noisy and needs to be modelled using the uncertainty of the true target s_t. Chen et al. [CAOH21] found that the uncertainty in perceiving the target's position in peripheral vision is linearly linked to the distance between the target and the current fixation position, referred to as eccentricity. Hence, $o_t \sim N(s, \sigma_o(t))$, where $\sigma_o(t) = \rho_{\text{spatial}} \times \text{eccentricity}(t)$. Here, $\rho_{\text{spatial}} = 0.09$, is a hyper-parameter of the model evaluated by Chen et al [CAOH21].

The transition function $T(s_{t+1}|s_t, a_t)$ between states in the RL environment can be set as constant, as the state of the environment stays the same in one episode, i.e. $s_{t+1} = s_t$. However, the belief of the agent about the environment state, i.e. the target position, needs to be updated at each time step, according to the new observation o_t. Chen et al. [CAOH21] initially set the belief of the agent to be a uniform distribution over all possible states. When the model takes action and fixates on a location, it receives a noisy estimate of where the target might be, which is used to update the belief and uncertainty about the target's position. After the first time step ($t = 1$), the belief b_t of the model about the target position is $b_1 = o_1$ and uncertainty $\sigma_b^2(t)$, of the target position is $\sigma_b^2(t = 1) = \sigma_o^2(t = 1)$. Both of the parameters are entirely based on the first observation. The belief update from the previous time step $b(t-1)$ to the current state $b(t)$ given the new observation o_t is demonstrated using the *Kalman filter* application in the following equations:

$$b(t) = b(t-1) + k_t \times [o(t) - b(t-1)] \tag{3.1}$$

$$\sigma_b^2(t-1) = \sigma_b^2(t-1) + k_t \times \sigma_b^2(t-1) \tag{3.2}$$

where k_t is the scaling factor introduced to ensure that the belief state is a valid probability distribution that integrates to 1 over all possible states. The value of k_t is computed as:

$$k_t = \frac{\sigma_b(t-1)^2}{\sigma_b(t-1)^2 + \sigma_o(t)^2} \tag{3.3}$$

To solve the described POMDP environment, Chen et al. [CAOH21] selected Proximal Policy Optimization (PPO). We follow their approach and use the belief space planning method [ZRTA21] to handle uncertainty in conjunction with PPO. The belief state planning algorithm keeps a probability distribution over the set of possible states, referred to as a belief state, which is updated based on the agent's observations and actions. Given its observations and past actions, the agent's belief state represents its current knowledge about the state of the environment. The following subsections explain the workflow of how reinforcement learning is implemented in detail.

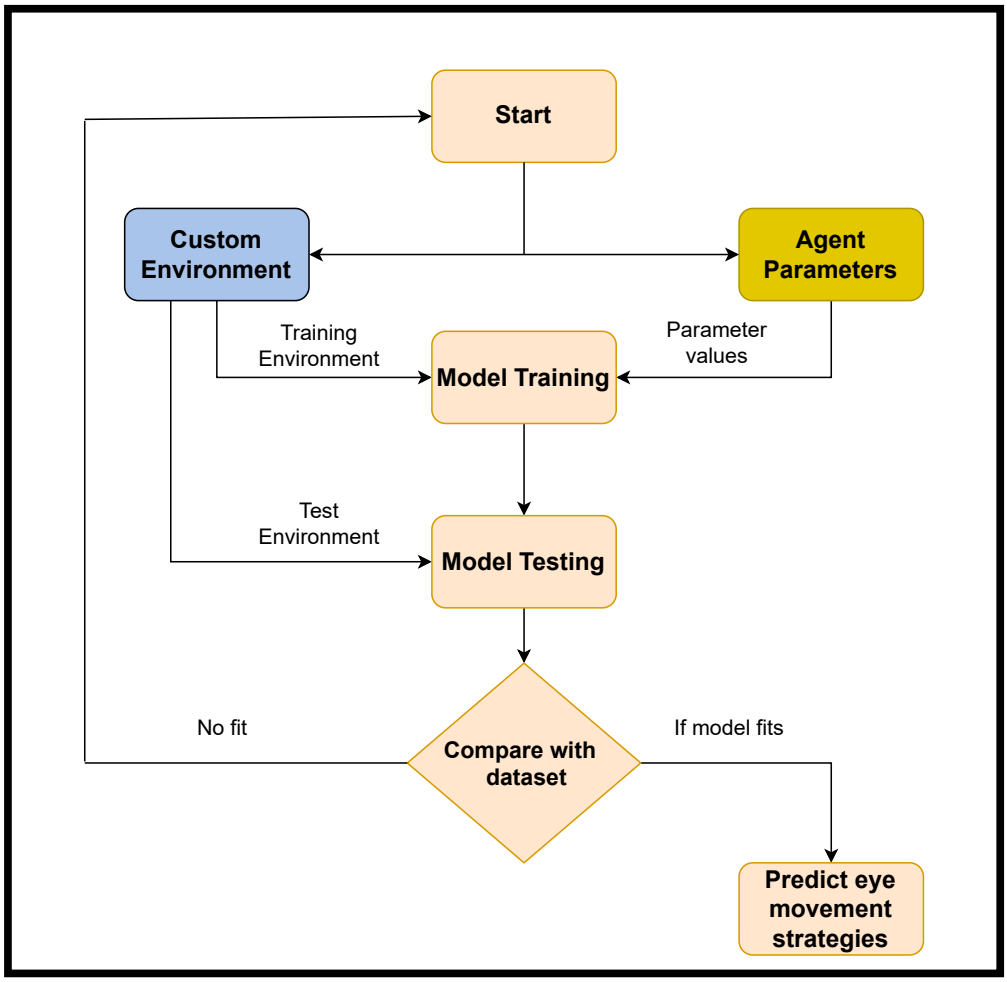

Figure 3.3: Flowchart of the training and testing process of the model using RL.

3.3 Model Computation

Figure 3.3 depicts the workflow of the RL process. As mentioned, the agent parameter values like oculomotor noise and visual-spatial noise were taken from the literature study by Chen et al. [CAOH21] and Zhang et al. [ZRZ10]. At first, an environment was implemented to generate training tasks (see Figure 3.4). The environment is a fundamental component of this project and was implemented from scratch to simulate the dynamics of human gaze-based selection strategies. It is implemented using Python [1] and leverages several essential libraries, including Gymnasium, a widely used toolkit for developing and testing reinforcement learning algorithms. The environment is built within OpenAI's Gymnasium [2] framework, which provides an easy-to-use interface for defining custom environments, actions, and observations. Our implementation incorporates the key parameters of the computational model defined earlier, e.g. the width of the target, distance from the starting position, ocular noise, and spatial noise. These parameters can be adjusted to mimic different scenarios and examine the impact of various factors on the gaze-based selection process.

For visualization and rendering, we utilize the Pygame library [3]. Pygame allows us to create a graphical display to visualize the interaction between the agent's gaze, the target, and the environment. This visualization is crucial for understanding the agent's behaviour and analyzing the outcomes of various strategies. Figure 3.4 represents the working of an episode in the environment. In this episode, the width of the target is 5° and the distance from the origin is 10°. The gaze starts from the origin and eventually reaches the target through a sequence of saccades and fixations. Figure 3.4 **(a)** denotes the first sequence and Figure 3.4 **(b)** represents the second and final sequence of the target selection.

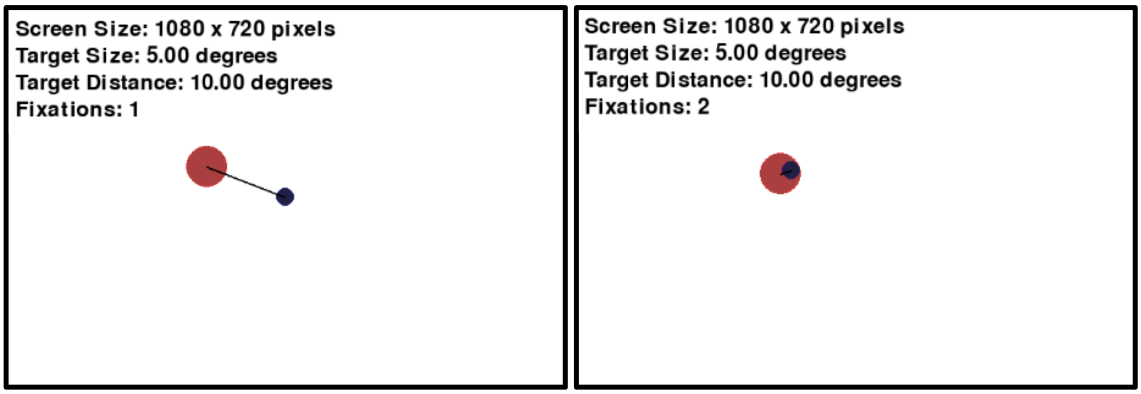

Figure 3.4: Example episode in the environment, where the red circle is the randomly selected target and the blue circle is the current gaze of the agent. Here, the episode starts with the first fixation at the centre of the screen **(a)** and concludes with the second fixation in target **(b)**.

[1] https://www.python.org/
[2] https://gymnasium.farama.org/index.html
[3] https://pypi.org/project/pygame/

The training process of the agent in the environment involves diverse combinations of target width W and distance D, as extracted from the research by Schuetz et al. [SMMZ19]. In each episode, a target was presented with varying sizes of visual angles, ranging from 1° to 5° of visual angle, positioned at distances of either 5° or 10° from the origin, randomly oriented at an angle θ. This training approach was outlined in the work of Chen et al. [CAOH21]. Conversely, we also tried training the agent with random initialization, providing insights into the model's adaptability under different initial conditions. For model refinement, we used the concept of epochs and batching. Within each epoch, width and distance combinations were intentionally shuffled to introduce variety into the training dataset. The agent's training was tailored to enable it to efficiently reach the target, aiming for minimal saccades and fixations. Once the training was done, the agent was tested on different combinations of target width and distance. Notably, the agent was not trained on human data rather it learned from the experience it gained during the interaction with our defined environment. Once tested, the agent's performance was compared with human data as mentioned in Figure 3.3. This includes analyzing factors such as the count of saccades for a specific width and distance combination, the duration of individual saccades, and other relevant metrics found in the human dataset [SMMZ19].

To extend the model introduced by Chen et al. [CAOH21], we developed a modified environment that incorporated fixational eye movements, also known as 'jitters'. When the initial saccade reached and fixated on the target, a continuous dwell time of 800 ms was mandated to finalize the target selection, following the work of Zhang et al. [ZRZ10]. During this dwell period, our gaze does not remain statically fixed on a single point; instead, it exhibits small, indistinct movements within an unspecified region, potentially causing the gaze to intermittently exit and re-enter the target area. To simulate this behaviour, we utilized the concept of the jitter average radius (AR) from Zhang et al. [ZRZ10], which correlated with target sizes. To determine the AR values, we employed linear regression on Zhang et al.'s findings and integrated the AR values into our model for various target sizes. The predicted AR values, namely $[0.13°, 0.15°, 0.18°, 0.24°, 0.27°, 0.29°]$ for corresponding target sizes $[1°, 1.5°, 2°, 3°, 4°, 5°]$, were integrated into our modeling approach.

Leveraging this AR, we randomly sampled points and adjusted our gaze's position to align with one of these sampled points. To optimize the utilization of this AR, we introduced Gaussian noise centred at zero with a standard deviation equal to the AR from the target position. This noise was applied to move the gaze to a new position. Equation 3.4 concisely describes this process. If this new position falls within the target region, the dwell time persists, allowing for further gaze shifts. However, if the gaze lands outside and re-enters the target region, the dwell time is reset to zero, initiating a fresh monitoring phase to maintain a continuous dwell time of 800ms. Finally, we determined the total target selection time by combining the Eye Movement Time (EMT), a minimum dwell time of 800ms, and the additional time required to reach this minimum dwell time due to the introduced jitters.

$$x_{\text{jitter}} = \sigma_{\text{jitter}} + x \tag{3.4}$$

where,

- σ_{jitter} is the standard deviation based on the AR.
- x is the current gaze position at each timestep.

Equation 3.5 illustrates the probability density function of the jitters sampled around the target region.

$$\sigma_{\text{jitter}} = \frac{1}{AR\sqrt{2\pi}} \cdot e^{-\frac{a^2}{2AR^2}} \tag{3.5}$$

where,

- AR is the Average Radius of the dwelling area.
- a is the target centre at each timestep.
- $e^{-\frac{a^2}{2(AR)^2}}$ is the exponent of Gaussian distribution describing the probability of jitter value influenced by AR.

In contrast to previous studies, our method offers a more authentic representation of human-like dwell time modelling. Unlike Chen et al. [CAOH21], who utilized a model devoid of jitter adjustments, and Zhang et al. [ZRZ10], who based their eye-pointing time modelling on the theoretical principles of Fitts' law, our approach accounts for real-world jitter adaptations.

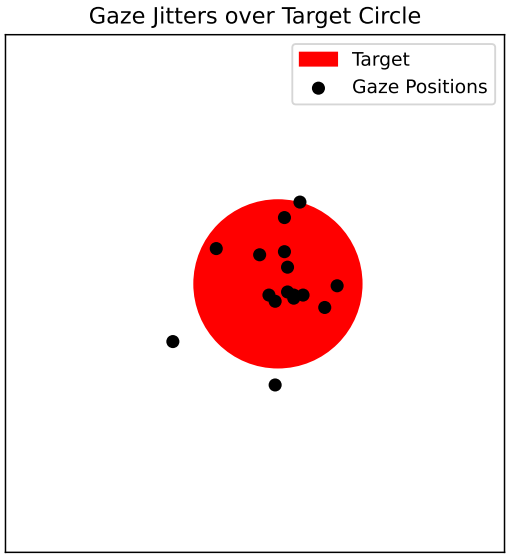

Figure 3.5: Plot of the forced gaze jitters confined within an Average Radius (AR) of 0.29° associated with the target size of 5°

.

In Figure 3.5, we illustrate the plotted distribution of induced jitters within the 5° target region. The average radius (AR) associated with this target size is 0.29°. It is notable that the AR decreases as the target size decreases [ZRZ10]. This empirical finding suggests that our gaze focuses on larger targets with less attention and, therefore, with a higher AR, and vice versa.

3.4 Model Evaluation

As mentioned in Figure 3.3, after these computations, when the model is trained, we compare our model's behaviour with the human data collected during experimental studies of Schuetz et al. [SMMZ19] and Zhang et al. [ZRZ10].

In the study by Schuetz et al. [SMMZ19], participants were tasked with executing eye movements from a designated starting point to a circular target. The starting positions of the gaze were indicated using a fixation cross and were recorded for 250 ms to establish a baseline for gaze accuracy and precision on a trial-by-trial basis. Following a randomized delay lasting between 250 ms and 1000 ms, a circular target was introduced. This target was placed at a 5° or 10° distance from the starting point, positioned randomly on a semicircle oriented towards the screen centre. Targets were presented with varying sizes (diameter of target circle: 0.5°, 1°, 1.5°, 2°, 3°, 4°, and 5°) in a randomized order. Trials were organized into blocks of 28, each encompassing combinations of seven target sizes, and two saccade amplitudes, and repeated twice. The gaze input device was an Eyelink 1000 plus video-based eye tracker at a sampling rate of 1000 Hz. The data from this study provides the required information about the number of saccades and the duration for individual saccades to make a target selection.

In the study by Zhang et al. [ZRZ10], each trial commenced with a fixation on a start button for 450 ms, with the start button randomly appearing at predefined positions. Subsequently, a group of five circular buttons, arranged in a 'plus' shape, appeared at a specified distance. Participants were instructed to quickly gaze at the central area of the desired target within the group, which was positioned at the centre. The target was positioned 6.13° away from the start button with the diameter of circles being 1.23°, 1.72°, 2.15°, 2.64°, and 3.07°. The eye tracking was facilitated using the Eye-Link II eye tracker, operating in pupil-only tracking mode, with a sampling rate of 250 Hz. The data from this study provides information about the factors influencing the dwell criterion. A detailed explanation of the comparative results is provided in the subsequent chapter.

4 Experimental Results

This section aims to elucidate the sequence of experiments and their outcomes, which involve comparing the behaviour of our model against datasets and the performance of the baseline model outlined in the study by Chen et al. [CAOH21]. The effective performance of our model stems from the careful design of the environment and meticulous selection of hyperparameters. The model's training unfolds through two key steps: Firstly, the interaction step entails the agent's engagement with the environment, taking actions and receiving rewards accordingly. Secondly, the learning step involves the agent being trained based on these rewards, with PPO clipping serving as the core objective function mentioned in equation 2.4. Throughout this research, the model's training occurred using various combinations of target width and distance. Over the course of 5 million timesteps, the model showcased evident convergence well before it reached the first million timestep milestone. However, it's noteworthy that certain scenarios emerged where the model struggled to attain convergence even after 5 million timesteps. These complexities will be thoroughly examined in the forthcoming 'Discussion' chapter.

The following sections describe the effects of target size and distance in the gaze-based selection task.

4.1 Effect of Target size

We examine the predictions of the number of saccades per trial in relation to varying target sizes. To this end, we compare the human data sourced from [SMMZ19], the baseline model discussed in [CAOH21], and the performance of our model implementation in Figure 4.1. The comparison demonstrates that our model's performance closely aligns with the predictions derived from the other sources for most target sizes. Notably, for larger target sizes, the number of saccades tended to be nearly one, while a clear upward trend in the number of saccades was evident as the target size decreased. For instances where the target size falls below 2°, our custom model exhibits slightly lower performance compared to the baseline model. This discrepancy is attributed to the fact that our model faced convergence challenges during training for these specific target sizes.

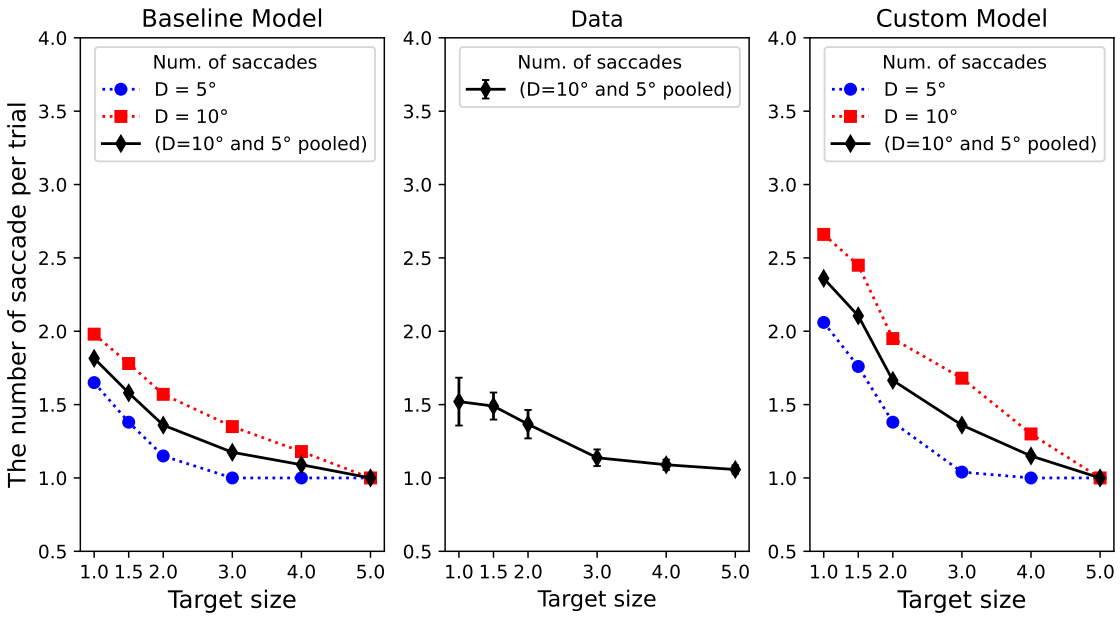

Figure 4.1: Effect of target size on the number of saccades. Left panel: Baseline model from [CAOH21]. Middle panel: Data plot from [SMMZ19]. Right panel: Plot from our custom model. The data points (represented by black circles) are consolidated from both the 10° distance condition and the 5° distance condition. The performance of the model is categorized based on target distance, indicated by orange squares for 10° distance and blue circles for 5° distance.

Target selection time as mentioned in Schuetz et al. [SMMZ19], did not incorporate a specific method of selection, such as a button press, to indicate the gaze being fixated on the target. Consequently, the authors established a more precise definition for selection time. The selection time was defined as the interval between the onset of the target and the moment when the gaze first entered the target area. To accommodate variations in eye tracker data, they determined the latter time point as the first instance within a 50 ms sliding window where all gaze samples were entirely within the target circle. Essentially, this approach captured the duration until the initial period of stable gaze on the target, irrespective of any detected eye movement events during this time window.

We adhered to the target selection time definition by Schuetz et al. [SMMZ19] and generated Figure 4.2. Comparing the performance of our model (right) to both the baseline model (left) and the data plot (middle) as shown in Figure 4.2, we can see that our model closely matches the effects found in human data and replicates the results of the baseline model by Chen et al. [CAOH21]. We can find the same phenomena, where the selection times (indicated by black circles) exhibit an upward trend as target sizes decrease, while the duration of individual saccades remains unaffected by the target size. This indicates that the increase in selection time primarily arises from the increased occurrence of secondary corrective saccades, particularly noticeable for smaller target sizes. Smaller and more distant targets are more likely to necessitate secondary saccades, resulting in the observed correlation between target size and selection time.

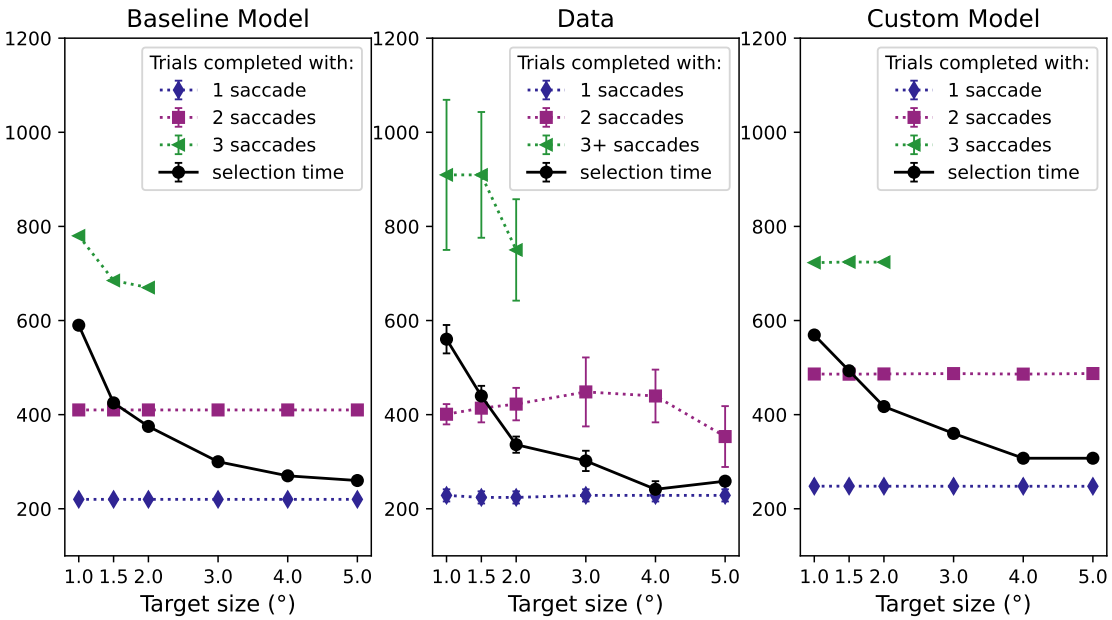

Figure 4.2: Effect of target size on selection time. Left panel: Baseline model plot from [CAOH21]. Middle Panel: Data plot from [SMMZ19]. Right panel: Selection time data from our custom model. Selection times are aggregated over both 5° and 10° distance conditions. Coloured lines indicate the saccade end times for the first, second and third saccades. Black circles indicate the overall selection time.

4.2 Effect of Index of Difficulty on the Number of Saccades

To assess the applicability of Fitts' Law [Fit54], a principle commonly used in pointing movements, we proceeded by computing the Index of Difficulty (ID) for each condition. The formula for calculating ID is mentioned in the equation 2.2. Subsequently, we plotted a graph to examine the relationship between these ID values and the number of saccades.

Figure 4.3 represents the plot of the number of saccades as a function of the Index of Difficulty. Research findings have consistently indicated a positive correlation between the Index of Difficulty (ID) and the length of saccadic sequences, aligning with Fitts' law [Min00]. Our model's analysis as shown in Figure 4.3 reveals that this trend is predominantly driven by the increased utilization of error-correcting secondary saccades, with their frequency rising as the distance to the target increases and diminishing as the target size decreases. In contrast to Fitts' Law, which predicts that movement time is a linear function of ID, our model predicts a divergence from this trend for cases where ID is below a specific threshold. Figure 4.4 depicts this process clearly. When the Index of Difficulty (ID) falls below a specific threshold (approximately 2 bits), our model predicts (Figure 4.4: right panel) that selection time becomes independent of ID. The rationale behind this observation is the elimination of the necessity for secondary or corrective saccades during these simpler selections (Figure 4.4: left panel). Specifically, the increase in the total number of saccades with the ID can be attributed to the heightened probability of secondary saccades at larger IDs. Meanwhile, the latency and duration of each primary saccade were found to be contingent on the amplitude. In essence,

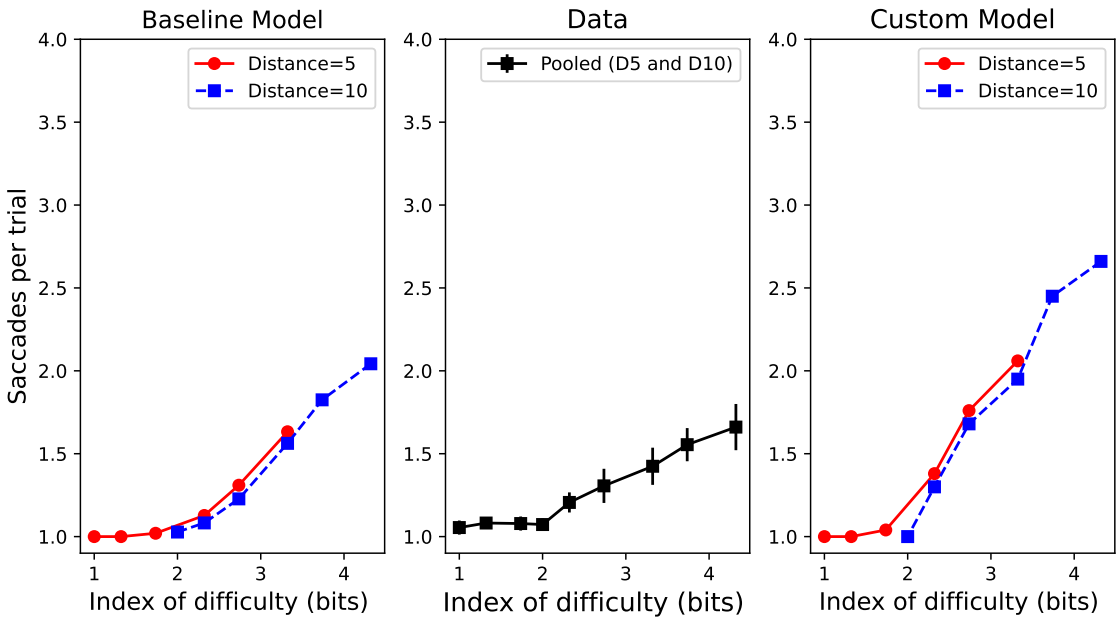

Figure 4.3: Number of saccades as a function of I.D. Left panel: Baseline model plot from [CAOH21]. Middle Panel: Data plot from [SMMZ19]. Right panel: I.D. plot from our custom model.

the task at hand requires only a primary saccade for accurate targeting, resulting in a decoupling of selection time from the usual linear relationship with ID, which is typically associated with Fitts' Law. Additionally, we employed regression analysis to determine the coefficients of Fitts' law. Fitting the Fitts' law curve described in equation 2.1 to the predicted movement time yielded the coefficients $a = 2.86ms$ and $b = 147.46ms$. A fundamental distinction exists between the outcomes of our model and those of other models that rely on Fitts' law. For instance, the models documented in [IAST18; Min00] do not incorporate the visual-spatial constraint into their modelling. In contrast, our model accounts for both oculomotor and visual-spatial constraints, potentially yielding divergent findings from theirs. The variance in our model's performance in contrast to the baseline model, particularly at bit 4, arose from the model's inability to converge for smaller target sizes.

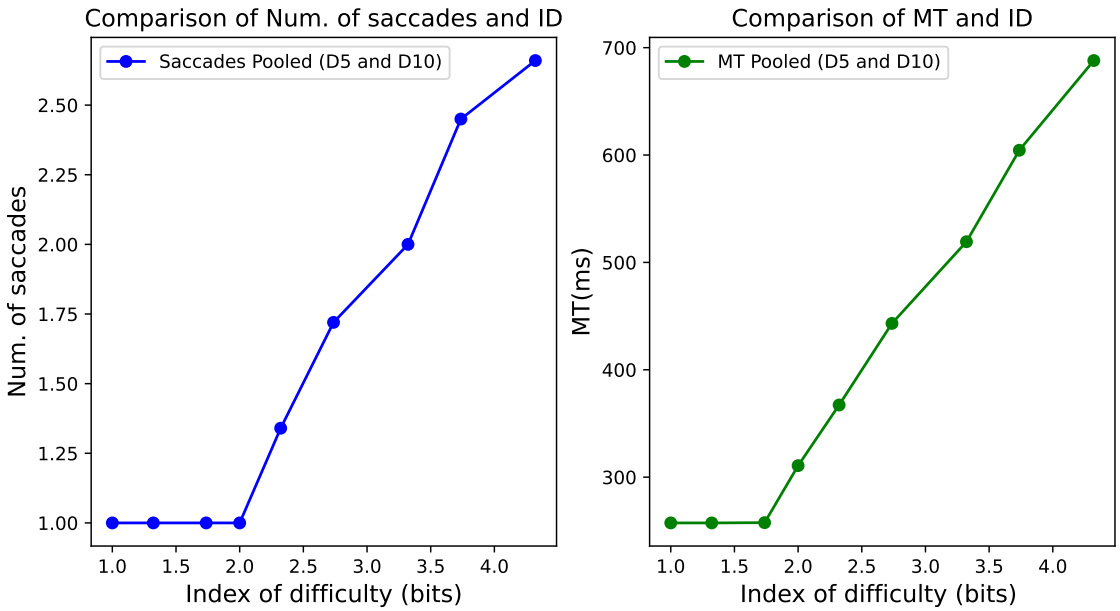

Figure 4.4: Comparison of MT and Number of saccades against ID.

4.3 Jitter Modelling

As highlighted earlier, in contrast to Chen et al. [CAOH21], our model incorporates adaptiveness to jitter and provides predictions for eye movement time and overall selection time. This was achieved by introducing a perturbation, relative to the Average Radius (AR) of the dwelling area [ZRZ10], to the gaze's position once it initially reaches the target and monitoring the time it takes for the gaze to reach the minimum dwell time of 800ms. Within each episode, we imposed a predetermined limit of eight shifts in gaze position, ensuring controlled and finite modelling conditions. The determination of this upper limit was based on iterative experimentation, demonstrating alignment with Zhang's data [ZRZ10] and superior performance compared to alternative values.

After establishing this upper limit, we conducted multiple model runs and calculated the average additional time required for each target size. Figure 4.5 illustrates the outcomes, depicting eye movement time (red bars) and dwell time with the added time required to meet the dwell criterion (blue bars). The plot clearly showcases an increase in dwell time as the target size decreases. For the smallest target (1°), our model took 1252ms for selection after the initial entry into the target region, exceeding the actual dwell criterion (800ms) by 452ms. This highlights that for larger target sizes, the gaze predominantly remains within the target area, while for smaller targets, the gaze tends to exit and re-enter more frequently, leading to significantly longer selection times.

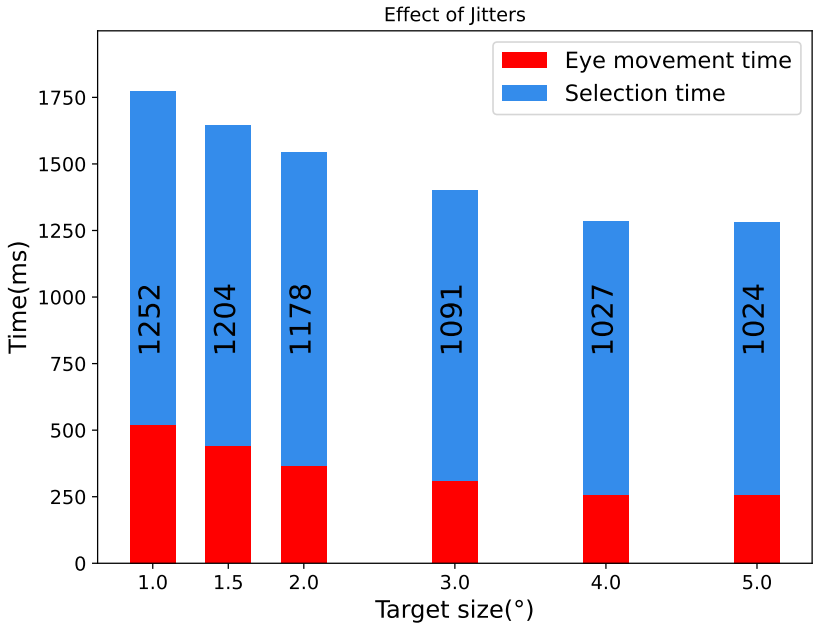

Figure 4.5: Effect of jitters on selection time. The graph illustrates the relationship between Eye Movement Time (EMT) and selection time in relation to the target size. EMT represents the duration from the initial appearance of the target to the point when the gaze first enters the target region. Selection Time encompasses EMT along with the minimum dwell time of 800ms in addition to the extra time required due to jitters.

5 Discussion and Conclusion

As highlighted in the preceding sections, we have formulated a computational model that successfully mirrors the performance of the baseline model introduced by Chen et al. [CAOH21]. The reported model is capable of predicting both aggregate-level data, such as selection time distributions, and detailed step-by-step gaze trajectories in gaze-based selection. The fundamental premise of our baseline model [CAOH21] is that the control policy is optimized based on utility, specifically selection time, within the constraints imposed by the visual and motor systems. This formulation transforms the problem into a POMDP, solvable through contemporary reinforcement learning methods, using algorithms like PPO. A noteworthy aspect of this approach is the emergence of human-like eye movements as a result of optimally bounded control. We were able the replicate the results of our baseline model. Therefore, we successfully implemented a computational model that allows an increased understanding of gaze-based selection processes.

Furthermore, we have investigated the applicability of Fitts' Law in gaze-based selection tasks, yielding a contrasting viewpoint. Our model's predictions diverge from Fitts' Law, which asserts that Movement Time (MT) in a target-directed movement task is proportionate to the ratio of movement amplitude and target size, quantified as an Index of Difficulty (ID). However, our model contends that below a specific threshold, the selection time becomes decoupled from the Index of Difficulty. We found, similar to Chen et al. [CAOH21], that this divergence arises from the absence of secondary or corrective saccades needed for simpler target selections. Ultimately, this indicates that Fitts' Law can only be a suitable model for gaze-based tasks when secondary or corrective saccades are involved.

A crucial aspect of our study revolves around the model training process, during which we explored two distinct methodologies. One approach involved the systematic exploration of width and distance combinations, allowing us to comprehensively analyze the model's performance across a spectrum of conditions. The second approach, in contrast, incorporated the method of random initialization, offering insights into how the model adapts when exposed to varying starting conditions. To fine-tune our model, we utilized the concept of epochs and batching. In each epoch, the width and distance combinations were deliberately shuffled to introduce diversity into the training dataset. This diversity ensured that the model developed robust patterns of gaze-based selection that could generalize across different scenarios. The training process proceeded through batches of these combinations, enabling efficient updates to the model.

It is important to note that despite training the model across a wide range of combinations, we observed that convergence was not achieved for certain scenarios, such as the instance where the width was 1° and the distance was 10°. This indicates that the model's performance is sensitive to specific combinations of width and distance, raising intriguing questions about the interaction between these parameters. In future work, we intend to focus on targeted training, refining specific combinations of width and distance and subsequently evaluating the model's performance against

other combinations. This focused exploration will help us understand the nuances and limitations of the model under specific conditions, further contributing to our understanding of gaze-based selection strategies.

In the later phase of our research, a significant stride was made by introducing "jitter adaptiveness" into the computational model. Our effort aimed to incorporate and simulate the concept of jitter. Unlike the approach by Chen et al. [CAOH21], where a fixed dwell time was employed, we computed the dwell time to mimic a human-like dwell behaviour. To model this human-like jitter behaviour, we enforced a jitter mechanism in our environment. Specifically, we introduced a strategy where the gaze, after entering the target region for the first time, was intentionally forced to "jitter" away from the precise target area. This deviation prompted the agent to re-engage with the target and continue the selection process, mimicking real-world scenarios where fine-tuning and corrective actions might be needed. To quantify the impact of this jitter strategy, we systematically evaluated its effect on the selection process. We calculated the additional time required by the gaze to align with the predefined dwell criterion, representing the period of stable fixation on the target. By doing so, we enhanced our model's ability to replicate human behaviour and provided valuable insights into possible real-world gaze interactions.

To summarize, our study has introduced a comprehensive model for gaze-based selection, one that demonstrates adaptability to a range of factors, including target size, width, and various sources of noise within the motor and vision systems. Furthermore, the model is designed to adapt to jitters. This model not only aligns with several significant empirical findings in the existing literature but also serves as a valuable foundation for driving future research endeavours. Our work bridges the gap between theoretical insights and practical applications, offering a holistic understanding of the dynamics of gaze-driven interactions. By capturing the essence of real-world complexities and providing a platform to explore and test hypotheses, our model extends its utility beyond the current study, making it a valuable tool for further investigations in this domain.

Bibliography

[BM08] N. J. Butko, J. R. Movellan. "I-POMDP: An infomax model of eye movement". In: *2008 7th IEEE International Conference on Development and Learning*. 2008 7th IEEE International Conference on Development and Learning. ISSN: 2161-9476. Aug. 2008, pp. 139–144. DOI: 10.1109/DEVLRN.2008.4640819 (cit. on pp. 13, 14).

[BRP18] J. Blattgerste, P. Renner, T. Pfeiffer. "Advantages of eye-gaze over head-gaze-based selection in virtual and augmented reality under varying field of views". In: *Proceedings of the Workshop on Communication by Gaze Interaction*. COGAIN '18. New York, NY, USA: Association for Computing Machinery, June 15, 2018, pp. 1–9. ISBN: 978-1-4503-5790-6. DOI: 10.1145/3206343.3206349. URL: https://doi.org/10.1145/3206343.3206349 (visited on 08/06/2023) (cit. on p. 11).

[BSKH75] R. W. Baloh, A. W. Sills, W. E. Kumley, V. Honrubia. "Quantitative measurement of saccade amplitude, duration, and velocity". In: *Neurology* 25.11 (Nov. 1, 1975), pp. 1065–1065. ISSN: 0028-3878, 1526-632X. DOI: 10.1212/WNL.25.11.1065. URL: https://www.neurology.org/lookup/doi/10.1212/WNL.25.11.1065 (visited on 08/06/2023) (cit. on p. 13).

[CAOH21] X. Chen, A. Acharya, A. Oulasvirta, A. Howes. "An Adaptive Model of Gaze-based Selection". In: *Proceedings of the 2021 CHI Conference on Human Factors in Computing Systems*. CHI '21. New York, NY, USA: Association for Computing Machinery, May 7, 2021, pp. 1–11. ISBN: 978-1-4503-8096-6. DOI: 10.1145/3411764.3445177. URL: https://dl.acm.org/doi/10.1145/3411764.3445177 (visited on 03/17/2023) (cit. on pp. 9, 12, 17, 18, 20–24, 27–31, 33, 34).

[CBB+15] X. Chen, G. Bailly, D. P. Brumby, A. Oulasvirta, A. Howes. "The Emergence of Interactive Behavior: A Model of Rational Menu Search". In: *Proceedings of the 33rd Annual ACM Conference on Human Factors in Computing Systems*. CHI '15. New York, NY, USA: Association for Computing Machinery, Apr. 18, 2015, pp. 4217–4226. ISBN: 978-1-4503-3145-6. DOI: 10.1145/2702123.2702483. URL: https://doi.org/10.1145/2702123.2702483 (visited on 08/06/2023) (cit. on p. 13).

[CG83] E. R. Crossman, P. J. Goodeve. "Feedback control of hand-movement and Fitts' Law". In: *The Quarterly Journal of Experimental Psychology A: Human Experimental Psychology* 35A.2 (1983). Place: United Kingdom Publisher: Taylor & Francis, pp. 251–278. ISSN: 1464-0740. DOI: 10.1080/14640748308402133 (cit. on p. 13).

[CSBH17] X. Chen, S. D. Starke, C. Baber, A. Howes. "A Cognitive Model of How People Make Decisions Through Interaction with Visual Displays". In: *Proceedings of the 2017 CHI Conference on Human Factors in Computing Systems*. CHI '17. New York, NY, USA: Association for Computing Machinery, May 2, 2017, pp. 1205–1216. ISBN: 978-1-4503-4655-9. DOI: 10.1145/3025453.3025596. URL: https://doi.org/10.1145/3025453.3025596 (visited on 08/06/2023) (cit. on p. 13).

[Duc18] A. T. Duchowski. "Gaze-Based Interaction: A 30 Year Retrospective". In: *Comput. Graph.* 73.C (June 2018), pp. 59–69. ISSN: 0097-8493. DOI: 10.1016/j.cag.2018.04.002. URL: https://doi.org/10.1016/j.cag.2018.04.002 (cit. on pp. 18, 20).

[Fit54] P. M. Fitts. "The information capacity of the human motor system in controlling the amplitude of movement". In: *Journal of Experimental Psychology* 47.6 (1954). Place: US Publisher: American Psychological Association, pp. 381–391. ISSN: 0022-1015. DOI: 10.1037/h0055392 (cit. on pp. 12, 29).

[FMK20] M. Fernandez, F. Mathis, M. Khamis. "GazeWheels: Comparing Dwell-time Feedback and Methods for Gaze Input". In: *Proceedings of the 11th Nordic Conference on Human-Computer Interaction: Shaping Experiences, Shaping Society*. NordiCHI '20. New York, NY, USA: Association for Computing Machinery, Oct. 26, 2020, pp. 1–6. ISBN: 978-1-4503-7579-5. DOI: 10.1145/3419249.3420122. URL: https://doi.org/10.1145/3419249.3420122 (visited on 08/06/2023) (cit. on p. 12).

[FR84] B. Fischer, E. Ramsperger. "Human express saccades: extremely short reaction times of goal directed eye movements". In: *Experimental Brain Research* 57.1 (Jan. 1, 1984), pp. 191–195. ISSN: 1432-1106. DOI: 10.1007/BF00231145. URL: https://doi.org/10.1007/BF00231145 (visited on 08/10/2023) (cit. on p. 18).

[GHT15] S. J. Gershman, E. J. Horvitz, J. B. Tenenbaum. "Computational rationality: A converging paradigm for intelligence in brains, minds, and machines". In: *Science* 349.6245 (2015), pp. 273–278. DOI: 10.1126/science.aac6076. eprint: https://www.science.org/doi/pdf/10.1126/science.aac6076. URL: https://www.science.org/doi/abs/10.1126/science.aac6076 (cit. on p. 9).

[GRGB18] J. Gori, O. Rioul, Y. Guiard, M. Beaudouin-Lafon. "The Perils of Confounding Factors: How Fitts' Law Experiments can Lead to False Conclusions". In: *Proceedings of the 2018 CHI Conference on Human Factors in Computing Systems*. CHI '18. New York, NY, USA: Association for Computing Machinery, Apr. 19, 2018, pp. 1–10. ISBN: 978-1-4503-5620-6. DOI: 10.1145/3173574.3173770. URL: https://dl.acm.org/doi/10.1145/3173574.3173770 (visited on 03/20/2023) (cit. on p. 9).

[HCAL18] A. Howes, X. Chen, A. Acharya, R. L. Lewis. "Interaction as an Emergent Property of a Partially Observable Markov Decision Process". In: *Computational Interaction*. Ed. by A. Oulasvirta, P. O. Kristensson, X. Bi, A. Howes. Oxford University Press, Jan. 18, 2018, p. 0. ISBN: 978-0-19-879960-3. DOI: 10.1093/oso/9780198799603.003.0011. URL: https://doi.org/10.1093/oso/9780198799603.003.0011 (visited on 08/06/2023) (cit. on pp. 13, 14).

[HLV09] A. Howes, R. Lewis, A. Vera. "Rational Adaptation Under Task and Processing Constraints: Implications for Testing Theories of Cognition and Action". English. In: *Psychological Review* 116.4 (Oct. 2009), pp. 717–751. ISSN: 0033-295X. DOI: 10.1037/a0017187 (cit. on p. 9).

[HRMB18] J. P. Hansen, V. Rajanna, I. S. MacKenzie, P. Bækgaard. "A Fitts' law study of click and dwell interaction by gaze, head and mouse with a head-mounted display". In: *Proceedings of the Workshop on Communication by Gaze Interaction*. COGAIN '18. New York, NY, USA: Association for Computing Machinery, June 15, 2018, pp. 1–5. ISBN: 978-1-4503-5790-6. DOI: 10.1145/3206343.3206344. URL: https://dl.acm.org/doi/10.1145/3206343.3206344 (visited on 03/20/2023) (cit. on pp. 9, 11).

[IAST18] T. Isomoto, T. Ando, B. Shizuki, S. Takahashi. "Dwell time reduction technique using Fitts' law for gaze-based target acquisition". In: *Proceedings of the 2018 ACM Symposium on Eye Tracking Research & Applications*. ETRA '18. New York, NY, USA: Association for Computing Machinery, June 14, 2018, pp. 1–7. ISBN: 978-1-4503-5706-7. DOI: 10.1145/3204493.3204532. URL: https://doi.org/10.1145/3204493.3204532 (visited on 08/06/2023) (cit. on pp. 12, 30).

[KH14] D. E. Kieras, A. J. Hornof. "Towards accurate and practical predictive models of active-vision-based visual search". In: *Proceedings of the SIGCHI Conference on Human Factors in Computing Systems*. CHI '14. New York, NY, USA: Association for Computing Machinery, Apr. 26, 2014, pp. 3875–3884. ISBN: 978-1-4503-2473-1. DOI: 10.1145/2556288.2557324. URL: https://doi.org/10.1145/2556288.2557324 (visited on 08/06/2023) (cit. on p. 13).

[LD10] R. Lin, C. Drury. "Modeling Fitts' law". In: Jan. 1, 2010 (cit. on p. 13).

[LHS14] R. Lewis, A. Howes, S. Singh. "Computational Rationality: Linking Mechanism and Behavior Through Bounded Utility Maximization". In: *Topics in Cognitive Science* 6 (Feb. 2014). DOI: 10.1111/tops.12086 (cit. on p. 9).

[LT15] R. F. Lin, Y.-C. Tsai. "The use of ballistic movement as an additional method to assess performance of computer mice". In: *International Journal of Industrial Ergonomics* 45 (Feb. 1, 2015), pp. 71–81. ISSN: 0169-8141. DOI: 10.1016/j.ergon.2014.12.003. URL: https://www.sciencedirect.com/science/article/pii/S016981411400170X (visited on 08/06/2023) (cit. on p. 13).

[MB14] P. Majaranta, A. Bulling. "Eye Tracking and Eye-Based Human–Computer Interaction". In: *Advances in Physiological Computing*. Ed. by S. H. Fairclough, K. Gilleade. Human–Computer Interaction Series. London: Springer, 2014, pp. 39–65. ISBN: 978-1-4471-6392-3. DOI: 10.1007/978-1-4471-6392-3_3. URL: https://doi.org/10.1007/978-1-4471-6392-3_3 (visited on 08/06/2023) (cit. on pp. 9, 12).

[Min00] D. Miniotas. "Application of Fitts' law to eye gaze interaction". In: *CHI '00 Extended Abstracts on Human Factors in Computing Systems*. CHI EA '00. New York, NY, USA: Association for Computing Machinery, Apr. 1, 2000, pp. 339–340. ISBN: 978-1-58113-248-9. DOI: 10.1145/633292.633496. URL: https://dl.acm.org/doi/10.1145/633292.633496 (visited on 08/06/2023) (cit. on pp. 13, 29, 30).

[QT17] Y. Y. Qian, R. J. Teather. "The Eyes Don't Have It: An Empirical Comparison of Head-Based and Eye-Based Selection in Virtual Reality". In: *Proceedings of the 5th Symposium on Spatial User Interaction*. SUI '17. Brighton, United Kingdom: Association for Computing Machinery, 2017, pp. 91–98. ISBN: 9781450354868. DOI: 10.1145/3131277.3132182. URL: https://doi.org/10.1145/3131277.3132182 (cit. on p. 9).

[Rao10] R. P. N. Rao. "Decision Making Under Uncertainty: A Neural Model Based on Partially Observable Markov Decision Processes". In: *Frontiers in Computational Neuroscience* 4 (Nov. 24, 2010), p. 146. ISSN: 1662-5188. DOI: 10.3389/fncom.2010.00146. URL: https://www.ncbi.nlm.nih.gov/pmc/articles/PMC2998859/ (visited on 08/06/2023) (cit. on p. 14).

[SJ00] L. E. Sibert, R. J. K. Jacob. “Evaluation of eye gaze interaction”. In: *Proceedings of the SIGCHI conference on Human Factors in Computing Systems*. CHI ’00. New York, NY, USA: Association for Computing Machinery, Apr. 1, 2000, pp. 281–288. ISBN: 978-1-58113-216-8. DOI: 10.1145/332040.332445. URL: https://dl.acm.org/doi/10.1145/332040.332445 (visited on 08/06/2023) (cit. on pp. 11, 13).

[SLM+17] J. Schulman, S. Levine, P. Moritz, M. I. Jordan, P. Abbeel. *Trust Region Policy Optimization*. Apr. 20, 2017. DOI: 10.48550/arXiv.1502.05477. arXiv: 1502.05477[cs]. URL: http://arxiv.org/abs/1502.05477 (visited on 08/07/2023) (cit. on p. 14).

[SMMZ19] I. Schuetz, T. S. Murdison, K. J. MacKenzie, M. Zannoli. “An Explanation of Fitts’ Law-like Performance in Gaze-Based Selection Tasks Using a Psychophysics Approach”. In: *Proceedings of the 2019 CHI Conference on Human Factors in Computing Systems*. CHI ’19. New York, NY, USA: Association for Computing Machinery, May 2, 2019, pp. 1–13. ISBN: 978-1-4503-5970-2. DOI: 10.1145/3290605.3300765. URL: https://dl.acm.org/doi/10.1145/3290605.3300765 (visited on 03/19/2023) (cit. on pp. 9–13, 15, 23, 25, 27–30).

[SWD+17] J. Schulman, F. Wolski, P. Dhariwal, A. Radford, O. Klimov. *Proximal Policy Optimization Algorithms*. Aug. 28, 2017. DOI: 10.48550/arXiv.1707.06347. arXiv: 1707.06347[cs]. URL: http://arxiv.org/abs/1707.06347 (visited on 08/06/2023) (cit. on p. 15).

[TBC17] B. Tatler, J. Brockmole, R. Carpenter. “LATEST: A model of saccadic decisions in space and time”. In: *Psychological Review* 124 (Apr. 2017), pp. 267–300. DOI: 10.1037/rev0000054 (cit. on p. 9).

[WKK10] C.-C. Wu, O.-S. Kwon, E. Kowler. “Fitts’s Law and speed/accuracy trade-offs during sequences of saccades: Implications for strategies of saccadic planning”. In: *Vision Research* 50.21 (Oct. 12, 2010), pp. 2142–2157. ISSN: 0042-6989. DOI: 10.1016/j.visres.2010.08.008. URL: https://www.sciencedirect.com/science/article/pii/S0042698910003858 (visited on 08/06/2023) (cit. on pp. 11–13).

[WM86] C. Ware, H. H. Mikaelian. “An evaluation of an eye tracker as a device for computer input2”. In: *Proceedings of the SIGCHI/GI Conference on Human Factors in Computing Systems and Graphics Interface*. CHI ’87. New York, NY, USA: Association for Computing Machinery, May 1, 1986, pp. 183–188. ISBN: 978-0-89791-213-6. DOI: 10.1145/29933.275627. URL: https://dl.acm.org/doi/10.1145/29933.275627 (visited on 03/21/2023) (cit. on p. 11).

[ZM07] X. Zhang, I. S. MacKenzie. “Evaluating Eye Tracking with ISO 9241 - Part 9”. In: *Human-Computer Interaction. HCI Intelligent Multimodal Interaction Environments*. Ed. by J. A. Jacko. Lecture Notes in Computer Science. Berlin, Heidelberg: Springer, 2007, pp. 779–788. ISBN: 978-3-540-73110-8. DOI: 10.1007/978-3-540-73110-8_85 (cit. on p. 11).

[ZMI99] S. Zhai, C. Morimoto, S. Ihde. “Manual and gaze input cascaded (MAGIC) pointing”. In: *Proceedings of the SIGCHI conference on Human Factors in Computing Systems*. CHI ’99. New York, NY, USA: Association for Computing Machinery, May 1, 1999, pp. 246–253. ISBN: 978-0-201-48559-2. DOI: 10.1145/302979.303053. URL: https://dl.acm.org/doi/10.1145/302979.303053 (visited on 08/06/2023) (cit. on p. 13).

[ZRTA21] D. Zheng, J. Ridderhof, P. Tsiotras, A.-a. Agha-mohammadi. *Belief Space Planning: A Covariance Steering Approach*. 2021. arXiv: 2105.11092 [cs.RO] (cit. on p. 21).

[ZRZ10] X. Zhang, X. Ren, H. Zha. "Modeling dwell-based eye pointing target acquisition". In: *Proceedings of the SIGCHI Conference on Human Factors in Computing Systems*. CHI '10. New York, NY, USA: Association for Computing Machinery, Apr. 10, 2010, pp. 2083–2092. ISBN: 978-1-60558-929-9. DOI: 10.1145/1753326.1753645. URL: https://dl.acm.org/doi/10.1145/1753326.1753645 (visited on 03/19/2023) (cit. on pp. 10, 18, 22–25, 31).

Declaration

I hereby declare that the work presented in this thesis is entirely my own. I did not use any other sources and references than the listed ones. I have marked all direct or indirect statements from other sources contained therein as quotations. Neither this work nor significant parts of it were part of another examination procedure. I have not published this work in whole or in part before. The electronic copy is consistent with all submitted hard copies.

---

place, date, signature